Pergamon

Int. J. Heat Mass Transfer. Vol. 39, No. 8, pp. 1729–1742, 1996

0017–9310/96 $15.00+0.00

0017–9310(95)00268–5

Convective heat transfer coefficients at a plane surface on a full-scale building facade

D. L. LOVEDAY and A. H. TAKI

Department of Civil and Building Engineering, Loughborough University, Loughborough, Leicestershire LE11 3TU, U.K.

(*Received* 18 *May* 1993 *and in final form* 23 *March* 1995)

Abstract—Accurate knowledge of the heat transfer processes at the external surfaces of buildings is necessary for design purposes. Using an experimental arrangement designed to provide measurements of good quality and accuracy, correlations are obtained for the external convection heat transfer coefficient h_c as a function of wind speed for a plane, smooth test surface on the facade of an eight-storey building. Values for h_c were correlated with wind speeds measured 1 m from the test surface and at 11 m above the roof. The correlations presented may be used for the prediction of h_c values for the central region of smooth, multi-storey building facades between fourth and eighth storey levels inclusive.

1. INTRODUCTION

At the external surfaces of buildings, heat transfer takes place via the processes of convection and radiation. While radiation heat loss is a function of surface temperature and emissivity, convective heat loss is a function of a number of variables, such as wind speeds and flow regimes, surface orientation and roughness. This makes difficult the accurate determination of thermal energy loss from a building, because of the variety of conditions that can prevail across the surface of any given building. For design purposes, therefore, standard values for surface thermal resistances have been adopted [1] for the situations described as 'sheltered', 'normal' and 'severe' exposure, the latter three conditions having been categorised in general terms [1]. For those parts of the building envelope that are well-insulated (such as walls and roofs in modern structures), the influence of the external surface resistance R_{so} on the overall thermal transmittance, or U-value, is small, and the currently available coarse data for R_{so} used in design might be acceptable. However, in certain situations, a more refined knowledge about R_{so}, and hence external convection coefficients, is necessary. One example where more detailed information would help includes rooms at the corners of buildings, where heat loss is increased due to higher wind speeds; a more important example, however, is for the case of the glazed parts of a building facade, especially the single-glazed elements since these are the principal contributors to fabric heat loss. For single glazing, the bulk of the thermal resistance is provided by the internal and external surface resistances, and detailed knowledge about convection coefficients for these circumstances is needed in order to enhance the accuracy of heat loss calculations. This is particularly important, since the use of glass as an integral part of the building envelope is already widespread and is increasing. Glazed structures such as atria are a prevalent feature of modern buildings, and refinements to heat transfer knowledge in this application area would aid understanding not only of their thermal behaviour, but also of the ventilation patterns taking place within them.

Previous work by Sharples [2], Ito *et al.* [3], Nicol [4] and Sturrock [5] has produced initial experimental data about the variation of the external convective heat transfer coefficient, h_c, as a function of wind speed and surface roughness for several full-scale building structures. The work to be described in this paper is aimed at providing further, full-scale, experimental data of a similar nature, but from an experimental arrangement designed to furnish data of improved quality and accuracy compared with that achieved by previous researchers in this field. The specific objectives of this study are:

(i) to present details of the enhanced experimental design;

(ii) for a flat, smooth, test panel mounted on a building facade, to measure the convection coefficients, to correlate them with local and roof top wind speeds, and to compare the correlations with those obtained by investigators in previous studies and

(iii) for the case of the flat, smooth test surface, to provide data for thermal modelling applications, together with correlations for use by designers, and also to discuss the implications for saving heat that is lost through glazing.

The work forms part of a wider study aimed at investigating the influence of framework geometry on convective heat loss from windows. In this context, achievement of the third objective stated above will provide a basis for comparison when disrupted surfaces are subsequently tested.

NOMENCLATURE

h_c	convection coefficient [W m^{-2} K^{-1}]
q_f	heat flux into the surface [W m^{-2}]
q_r	long-wave radiation input to the surface [W m^{-2}]
q_s	solar irradiance incident upon the surface [W m^{-2}]
T_o	outside air temperature [K]
T_s	panel surface temperature [K]
T_{sky}	sky temperature [K]
V	local windspeed at building surface [m s^{-1}]
V_r	roof-top wind speed [m s^{-1}]
V_s	near-surface wind speed [m s^{-1}] (the velocity component principally in the horizontal plane)
V_{10}	wind speed measured 10 m above the ground [m s^{-1}].

Greek symbols

α_s	solar absorptance of the surface, dimensionless
ε	long-wave emittance of the surface, dimensionless
σ	Stefan–Boltzmann constant [5.6697×10^{-8} W m^{-2} K^{-4}].

2. THEORETICAL BASIS

In steady-state conditions, the heat balance at the exterior surface of a building requires that the rate of heat gain is equal to the rate of heat loss. This balance must be maintained between the heat flux from inside the building and the convective and radiative losses at the external surface to the atmosphere. Consider a flat panel mounted on the external surface of a building; in steady-state conditions, heat storage in the panel and evaporation terms can be neglected, and the net energy balance can be expressed as:

$$q_f + \alpha_s q_s + \varepsilon q_r = \varepsilon\sigma T_s^4 + h_c(T_s - T_o). \quad (1)$$

If measurements are made during the night, the effect of solar radiation can be avoided, offering the advantage that control of the temperature difference between the panel surface and the air temperature is rendered less complicated. The net radiation exchange with the environment includes:

(i) radiation input to the building from the ground surface, other buildings, and the sky in the form of long-wave emission from these surfaces, and is equal to:

$$\varepsilon q_r = \varepsilon\sigma T_{sky}^4 \quad (2)$$

where T_{sky} is the sky temperature in Kelvin and can be approximated as [6]:

$$T_{sky} = T_o - 6 \quad (3)$$

(ii) the long-wave radiation loss from the external surface; equation (1) can therefore be simplified to yield:

$$q_f = h_c(T_s - T_o) + \varepsilon\sigma\left(T_s^4 - T_{sky}^4\right) \quad (4)$$

or

$$h_c = \frac{q_f - \varepsilon\sigma(T_s^4 - T_{sky}^4)}{(T_s - T_o)}. \quad (5)$$

Equation (5) is used to calculate the convection coefficient, h_c, in these studies.

3. PREVIOUS FULL-SCALE WORK

Sharples [2] and Ito [3] each used a very similar experimental set-up to the other, in their measurements of surface heat transfer coefficients. This consisted of supplying two slightly different heat flow rates to two external copper plates so as to eliminate the necessity to measure radiation exchange. To aid our experimental design, an analysis was carried out which showed that the overall uncertainty in the convection coefficient for the case of using a two-panel system is higher than that for the case of a single panel system. By using two panels, the chief contribution to the overall uncertainty in h_c is made by the uncertainty in the two panel surface temperatures with the possibility of large errors occurring because of the fourth power dependencies. It was therefore decided that, in our study, a single panel would be used. Even allowing for up to a 30% error in the value for the long wave radiation input (which includes T_{sky}), the use of one panel still provides for reduced uncertainty in h_c as compared with values obtained from two panels.

The ASHRAE Task Group [7] has incorporated the results of Ito [3] in a general series of algorithms for energy calculations by stating that:

$$h_c = 18.6V_s^{0.605} \quad (6)$$

where h_c is in W m^{-2} K^{-1} and V_s is in m s^{-1}. Here, V_s is the wind speed measured at 0.3 m from the external surface and is given by:

$$V_s = 0.25V_{10} \quad (7)$$

for windward surfaces and $V_{10} > 2$ m s^{-1}, and

$$V_s = 0.05V_{10} + 0.3 \quad (8)$$

for leeward surfaces. Here, V_{10} is the wind speed measured at a height of 10 m above the ground.

Sharples [2] suggested the following formulae for his convection coefficient measured at the edge of the 18th floor of a 78 m high slab-type building in Sheffield city centre, U.K. For windward and leeward surfaces:

$$h_c = 1.7V_s + 5.1 \quad (9)$$

where V_s is the windspeed measured at 1 m from the external surface.

Measurements at the central site of the 18th floor gave the following correlations. For windward surfaces:

$$h_c = 1.4V_{10} + 6.5 \quad (10)$$

and, for leeward surfaces:

$$h_c = 1.4V_{10} + 4.4. \quad (11)$$

The CIBS Guide [8] gives the following expression for calculating the forced convection coefficient:

$$h_c = 4.1V + 5.8 \quad (12)$$

where V is described as the local wind speed at a building surface in m s^{-1}.

Nicol [4] examined the energy loss from an exterior window surface at Inuvik, Canada. His derived regression equation is:

$$h_c = 4.35V_r + 7.55 \quad (13)$$

where V_r is the roof-top wind speed, m s^{-1}.

Sturrock [5] suggested that, for a surface of average exposure:

$$h_c = 6.0V_r + 5.7 \quad (14)$$

where V_r is defined as above.

It can be seen that a number of differing correlations already exist in the literature. One purpose of our study is to provide further experimental data of enhanced quality and accuracy, and to compare results with previous work. In this respect, the design of the experimental arrangement is important, and is described next.

4. EXPERIMENTAL DESIGN AND PROCEDURE

4.1. *Location of building*

Rectangular buildings with sharp edges produce flows which cause high turbulence and recirculation. Buildings of this shape are common, however, and so experimental results from such buildings will be of general application. A suitable building for the present study was made available at the campus of Loughborough University of Technology, U.K. This was the eight-storey Whitworth building, a student hall of residence, and full-scale measurements were made on one of its facades. The ground floor of the building is L-shaped in plan while the remaining floors are rectangular in plan, and are of dimensions 21 m long × 9 m wide; the total height of the building is 28 m. It stands on slightly sloping ground and protrudes above the neighbouring roof levels in a semi-urban environment. This is shown in Fig. 1, an aerial photograph.

Figure 2 is a plan showing the location of the study building in relation to structures in its immediate vicinity. The south-east (SE) wall of the building was chosen for this study because it was a relatively flat, undisrupted surface as compared with the other facades of the building; in addition, it is subject to windward flow. Identification of the predominantly windward direction was based on wind data measured at 10 m height above the ground at Newtown Linford, Bradgate Park, a weather station 8 km south of the campus. The north and west facades of the building face an open square, while the south and east facades face low-rise buildings which afford some shelter.

4.2. *The test panel*

The chosen test facade consisted of a brick wall. An aluminium rail channel was fixed to the wall, and the test panel of dimensions 0.8 m wide × 0.5 m high was designed so as to slide vertically in the channel by means of wheels. By lowering the panel from the flat roof of the building, the panel comes to rest in a rectangular framework at floor level six. The rail and framework were secured by bolts to the wall. Air flow ramps were attached to the framework and have been designed so as to minimise any step effect on the air flowing over the panel. The panel was pulled up and down manually via a nylon rope; Fig. 3 is a photograph of the panel/rail arrangement.

For reasons described in Section 3, a single test panel system was adopted. The test panel and its heating system were housed within a rectangular polypropylene box, measuring 842 mm wide × 530 mm high by 65 mm deep. Figure 4 shows a section of the panel unit. The panel contains a 240 V a.c. electric heater mat of output power 1 kW m^{-2} supplied by the Jimi-Heat Company; this particular heater mat was chosen because it is thin, and offers both exceptional flexibility and uniformity of heat flux. The heater was installed between a 1 mm thick aluminium plate and a 2 mm thick internal copper plate, so as to provide a uniform heat flow for detection by a heat flux meter. A Variac transformer was used to control the heat flux. The heat flux meter was designed, built and supplied by the University of Lille, France; it consists of an electroplated thermopile 0.8 m wide, 0.5 m high and of less than 1 mm thickness; it has a calibrated output of 380 μV W^{-1} m^{-2}, giving a high degree of sensitivity, uniformity and repeatability. This device was placed between the internal copper plate and a second 2 mm thick external copper plate. The latter comprised the outermost surface of the test panel, which was exposed to the external environment and painted with 'Nextel' 7007 primer prior to the application of a 'Nextel' 2010 top coat. This was to ensure a smooth black paint finish with an experimentally tested absorptance of 0.95–0.98. Nine platinum resistance thermometers were attached to recesses drilled in the non-exposed side of the copper plate. The sen-

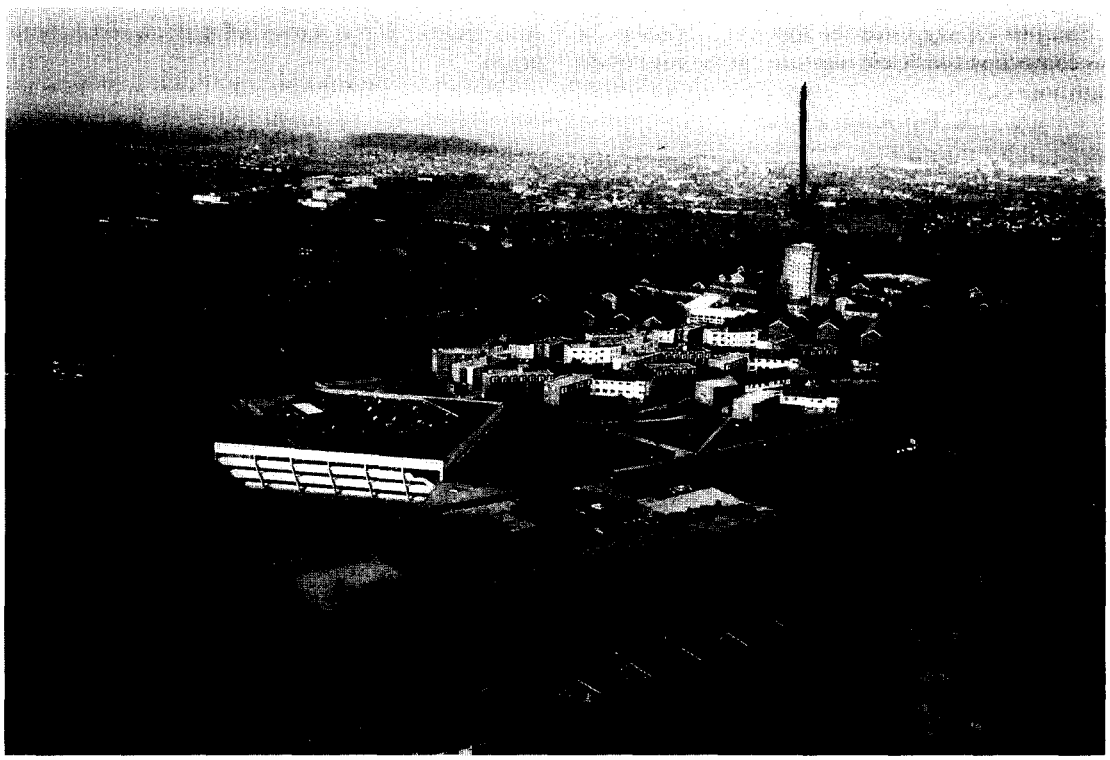

Fig. 1. Aerial photograph showing Whitworth Building and its surroundings.

sors were connected in series-parallel loops for measuring the average external surface temperature of the panel. In order to provide good thermal contact between each element in Fig. 4, heat transfer paste was used, and in order to reduce edge heat losses the test panel unit was insulated at the rear and sides.

4.3. *The mast*

A mast for measuring roof wind speed and direction was constructed as shown in Fig. 5, using aluminium alloy tube of diameter 6.4 cm and wall thickness 0.64 cm. Two sections of tube each of 5 m length were joined by means of fixing couplings and secured by bolts. A quick-clamp socket was fixed at the top of the mast to reduce the tube diameter to 2.54 cm, where a combined anemometer and wind vane were mounted via a cross-arm. The anemometer was the A100R switching type, the wind vane was the W200P potentiometer type, and both were supplied by Vector Instruments. In determining the length of the mast, the distance above the roof level to which the building influences the wind flow needs to be estimated; the most important factor in this estimation is the surface area of the windward facade. For the Whitworth Building it was estimated that 11 m is the height required above the roof level so as to record undisturbed flows. The 10-m long mast was attached one metre above the roof level to the wall of the data logging room by means of three mounting brackets distributed along its support length. In addition, four guy wires each of 6 mm thickness were used to support the mast. The structural safety of the entire design and fittings (mast, rail, panel and framework) were checked and approved by an independent consultant.

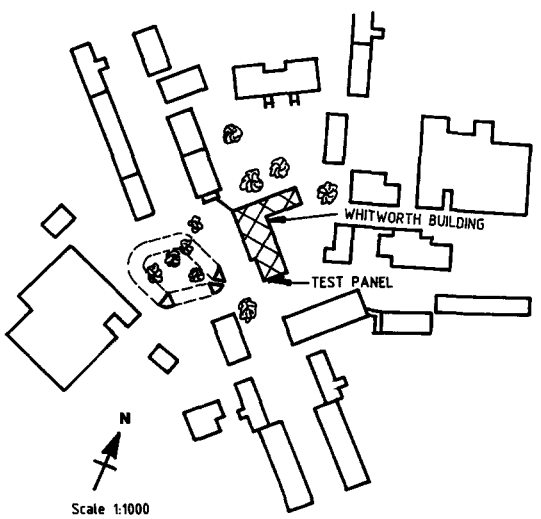

Fig. 2. Plan of Whitworth Building and nearby structures.

4.4. *Surface wind speed measurement*

Airflow around buildings in the atmospheric boundary layer is complicated and erratic, the building interacting strongly with the oncoming wind to produce regions consisting of separation cavities and

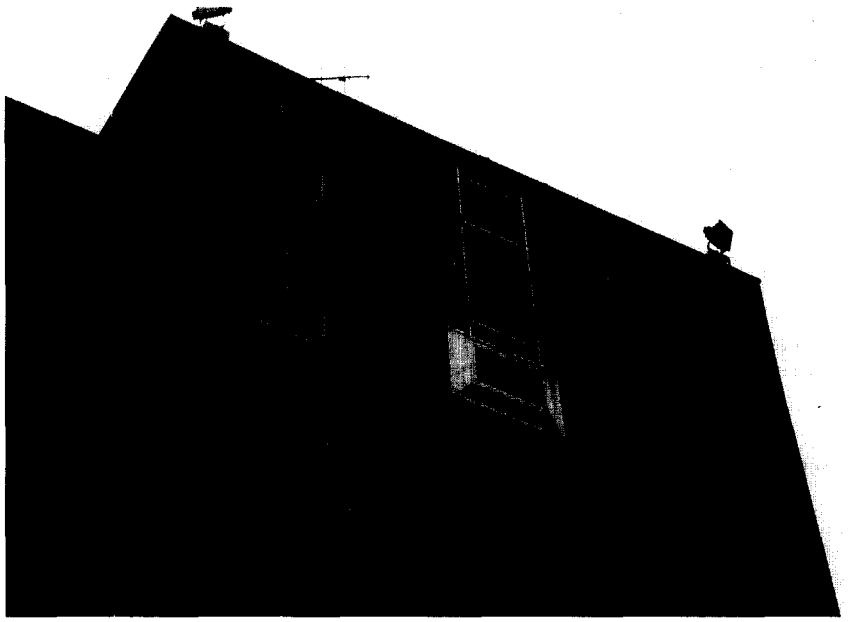

Fig. 3. Photograph of the test panel and rail system.

vortices. This complexity of the airflow pattern around building surfaces produces a very difficult situation as regards measurement of velocities close to the surfaces, requiring sophisticated and expensive equipment if accurate results are to be achieved. In addition, such equipment must respond to the airflow no matter which direction it takes, and should be sufficiently portable and lightweight to enable it to be supported safely. Yet, it must be designed for outside use and thus be rugged enough to survive the hostile operating conditions. After a lengthy survey of available equipment, it was decided to use a Gill Ultrasonic Anemometer supplied by Biral. This consists of a sensing head with six transducers arranged in three pairs, surrounding a cylindrical electronic base housing (see Fig. 6), for measuring both the wind speed and its direction; in-built electronics provide all processing and vector computations required for outputting wind data in analogue and serial data formats.

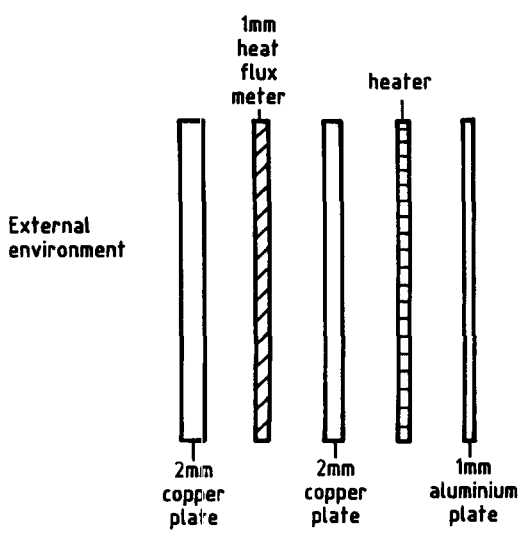

Fig. 4. Cross-section of test panel unit.

The instrument was mounted vertically at 1 m from the external surface of the building by means of a bracket fixed near the test panel. Outside air temperature was measured using a standard platinum resistance thermometer housed within a waterproof terminal box; its sensing element was additionally enclosed inside a protruding protective tube attached to the anemometer bracket.

4.5. *Data logging*

Simultaneous monitoring was required of the ten different signals provided by the thermal and airflow measuring equipment. This was achieved using a Campbell Scientific Instruments 21X micro logger and M416 multiplexer. Signals were sampled at 10 s intervals and then average values calculated every 5 min. Each night's measurements produced ten signals logged every 10 s for 12 hours, giving 43 200 pieces of information. At the end of each night's run, these data were downloaded into a lap-top computer for processing. Computer programmes were developed to read the data and to calculate 5-min averaged values. These values were converted to engineering units and classified into two categories:

(a) windward; when the wind incidence angle lies between 0° and 180° inclusive to the front of the panel (see Fig. 10).

(b) leeward; for all other directions.

4.6. *Experimental procedure*

All measurements were made at the central site, sixth-floor level, of the south-east facade of the Whitworth building. A consistent procedure was carried

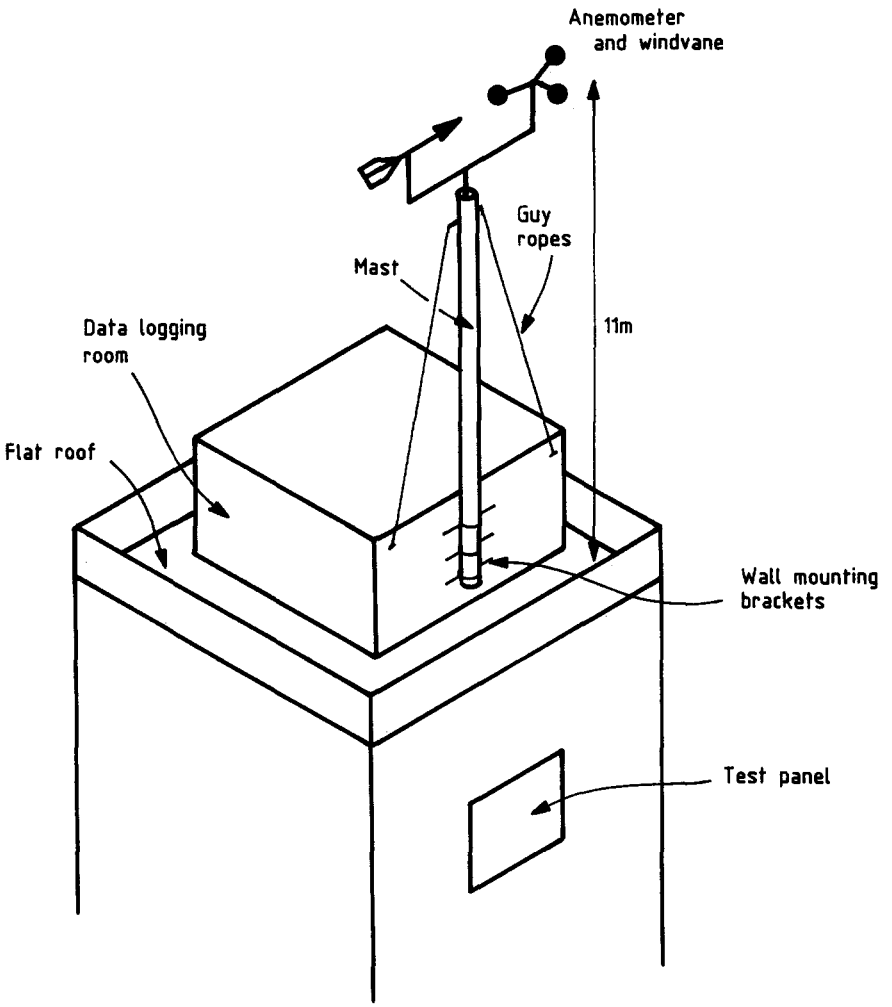

Fig. 5. Illustration of mast and its position relative to the test panel.

out prior to the commencement of each night's experiment. This comprised:

(i) an inspection of the entire system constructed to ensure that every item was secure, since safety is one of the most important aspects in the design of the system;
(ii) a check of the output signals to ensure fault-free operation of the system;
(iii) adjustment of the Variac transformer to control the heater output for a 2-h 'settling period' prior to the commencement of logging.

5. EXPERIMENTAL FINDINGS

5.1. *Results involving* V_r

Figures 7 and 8 illustrate, for windward and leeward conditions respectively, the fluctuations of the net long-wave radiation, q_r, panel surface temperature, T_s, and roof wind speed, V_r, over one night. The graphs of long-wave radiation emission and panel surface temperature appear 'in phase', showing that long-wave radiation emission is directly proportional to panel surface temperature. The graphs of panel surface temperature and wind speed (measured at roof level) appear 'in anti phase'. These findings show that as wind speed increases convection becomes the dominant mode of heat loss; as the wind speed decreases, radiation heat transfer takes over as the dominant mode.

Figure 9 shows the variation of the convection coefficient h_c as a function of wind direction, Θ degrees, for three ranges of roof windspeed, V_r (Fig. 10 defines the wind direction with respect to the test panel). Inspection of Fig. 9 (together with individual plots (not shown) for the three separate ranges of V_r) revealed the following effects.

(i) The peaks between 0 and 20° and between 125 and 150° are due mainly to higher wind velocities (the peaks disappearing at lower windspeeds). (Sharples [2] also found peaks in his value for h_c between 140 and 160°.)

(ii) The peak between 65 and 80° is due mainly to

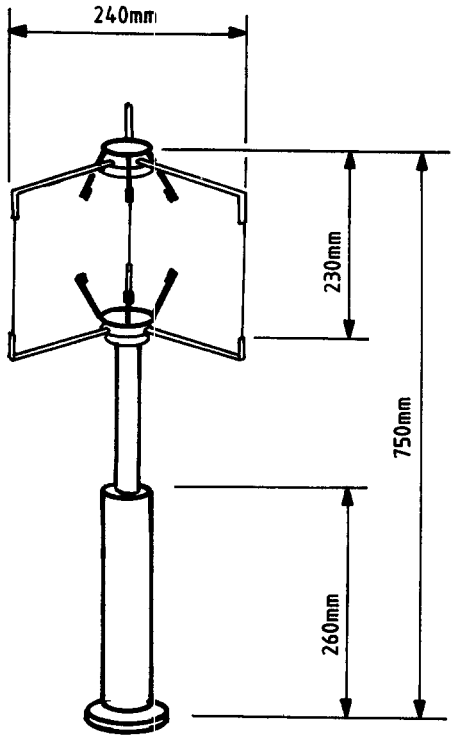

Fig. 6. the ultrasonic anemometer.

wind direction (the peak being present over a wide range of velocities).

(iii) At 90°, the value for h_c is low across all velocities, since this incidence angle corresponds to the condition of stagnation flow.

(iv) When the wind strikes the rear surface of the building (range 181°–359°) the convection coefficients are relatively low, as expected from the sheltering effect of the building.

Though further information about the effect of wind direction on h_c could be extracted from the recorded data, it must be emphasised that the overriding objective of the present study is to investigate the effect of wind velocities on h_c as specified into 'windward' and 'leeward' categories only, as an aid to design and for comparison with other studies. The results presented here are therefore average correlations, based on the full set of measured values, without directional weighting.

Figures 11 and 12 show the variation of the convection coefficient h_c with roof wind speed V_r for windward and leeward conditions respectively, together with the corresponding least-squares linear correlation equations to the data. It is clear that h_c increases with the increase of V_r for both windward and leeward conditions. However, the points are more scattered in Fig. 11 (for the windward conditions) than in Fig. 12 (for the leeward conditions), particularly at higher windspeeds. This is thought to be caused by variations in wind direction, especially at the higher speeds (Fig. 9). Windward flows are particularly affected by this. Categorising the data on wind speed direction into bands, say 30° in width, could lead to reduced scatter. This has not been carried out to date in the present study for the reasons of utility to designers as stated earlier; besides this, larger datasets would be necessary for a comprehensive treatment.

Linear regression gives, for the windward condition (correlation coefficient $r = 0.63$):

$$h_c = 2.00V_r + 8.91 \tag{15}$$

and for the leeward conditions ($r = 0.82$):

$$h_c = 1.77V_r + 4.93 \tag{16}$$

where V_r is the wind speed measured (11 m above the roof level) in the free stream.

Equations (15) and (16) are useful for design purposes because V_r was measured in the free stream

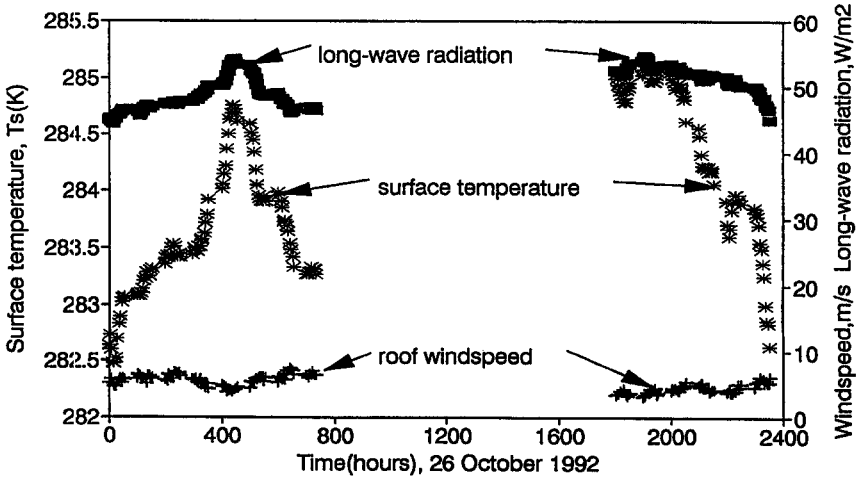

Fig. 7. Variation over time of net longwave radiation q_r, panel surface temperature T_s and roof wind speed V_r for windward conditions.

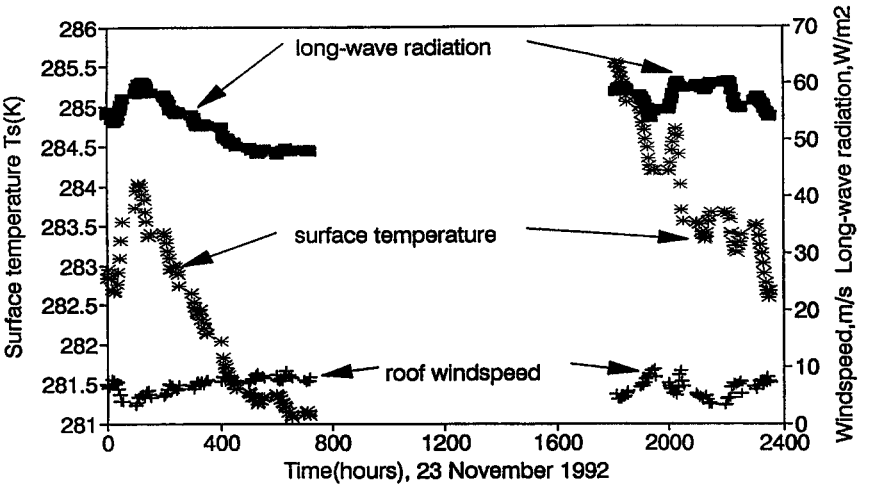

Fig. 8. Variation over time of net longwave radiation q_r, panel surface temperature T_s and roof wind speed V_r for leeward conditions.

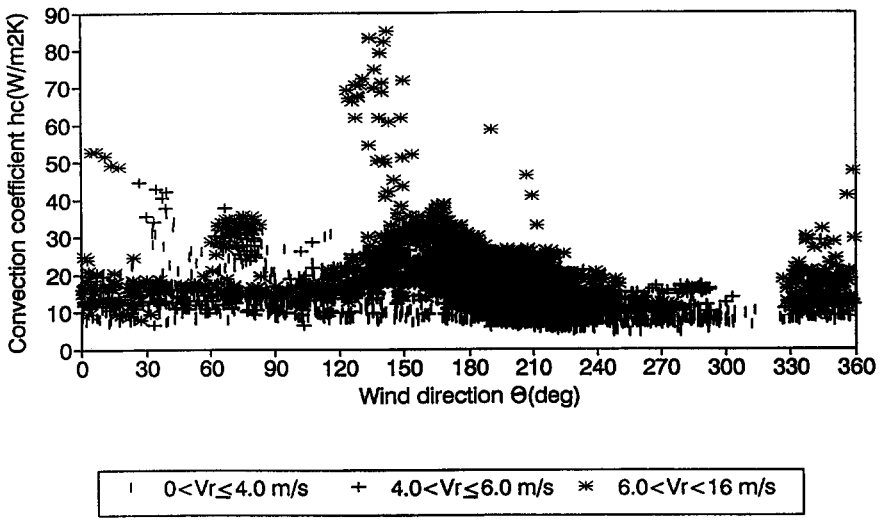

Fig. 9. Convection coefficient h_c vs wind direction Θ for various ranges of V_r.

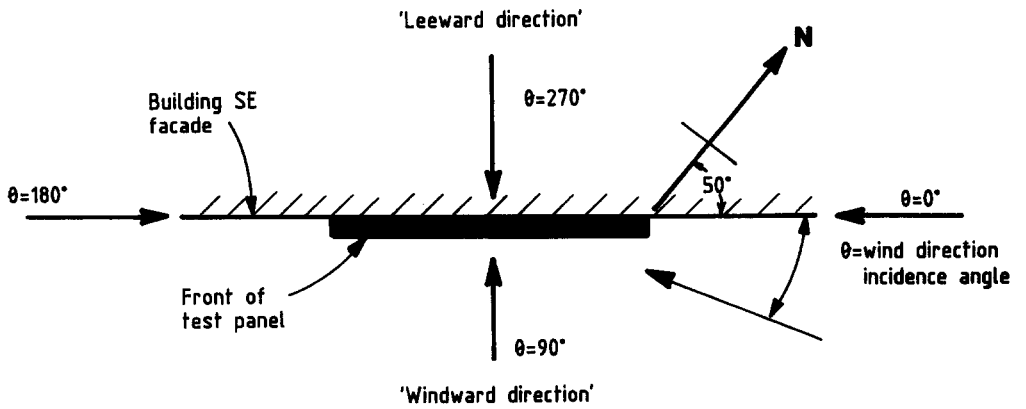

Fig. 10. Plan view of the test panel showing convention for wind direction.

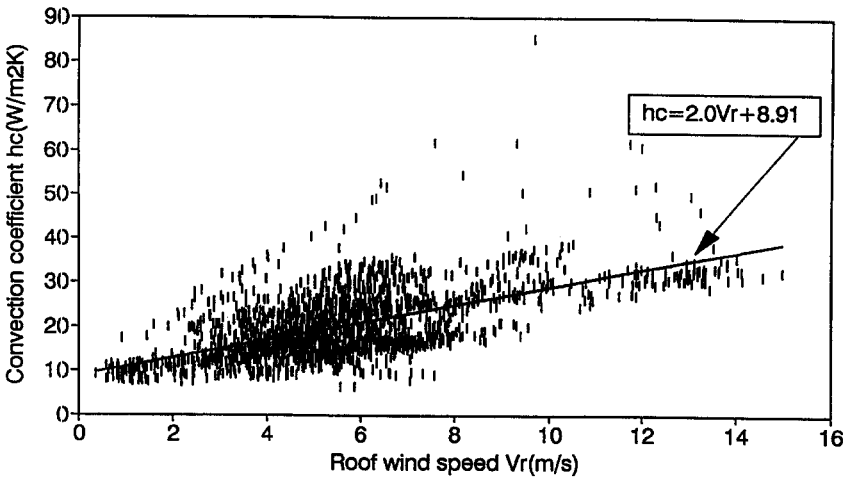

Fig. 11. Convection coefficient h_c vs roof wind speed V_r for windward conditions.

condition; the latter condition can be found by designers for other buildings, thus permitting the correlations to be applied in other situations.

5.2. *Results involving* V_s

Where local flow conditions around a building are known, equations (17) and (18) which follow can be used to more accurately estimate a value for h_c. Here, h_c is presented as a function of V_s, the wind speed measured at 1 m from the test panel surface. It is necessary to define V_s in more detail. The ultrasonic anemometer (Fig. 6) was used to measure the velocity vector (windspeed and direction) defined as the resultant of the horizontal (x-plane) component and the vertical (y-plane) component. Note that the 'x-plane' is taken as the horizontal plane perpendicular to the building facade, while the 'y-plane' is the vertical plane parallel to the facade. A correlation (not shown) for h_c vs V_{sx} was derived, where V_{sx} is the velocity component in the x-plane only; this revealed almost no change to the plots already obtained for h_c vs V_s. It is concluded therefore, that the velocity vector V_s as measured and presented throughout this paper is predominantly the velocity component in the horizontal plane (i.e. $V_s \approx V_{sx}$). (The term 'windspeed' used in this paper for V_s implies speeds measured in the x-plane.)

The variations of h_c with the wind speed V_s measured at 1 m from the panel surface are shown in Figs. 13 and 14 for windward and leeward conditions, respectively. The data again show less scatter for the case of leeward conditions. Polynomial regression gives, for the windward conditions ($r = 0.76$):

$$h_c = 16.15 V_s^{0.397} \tag{17}$$

and for the leeward conditions ($r = 0.82$):

$$h_c = 16.25 V_s^{0.503}. \tag{18}$$

The average correlation for combined windward and leeward conditions is:

$$h_c = 16.21 V_s^{0.452}. \tag{19}$$

In general, values for h_c for the leeward conditions

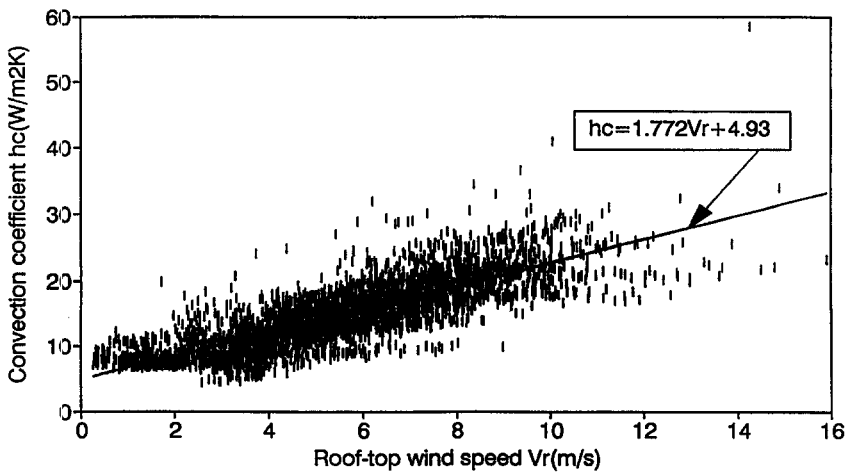

Fig. 12. Convection coefficient h_c vs roof wind speed V_r for leeward conditions.

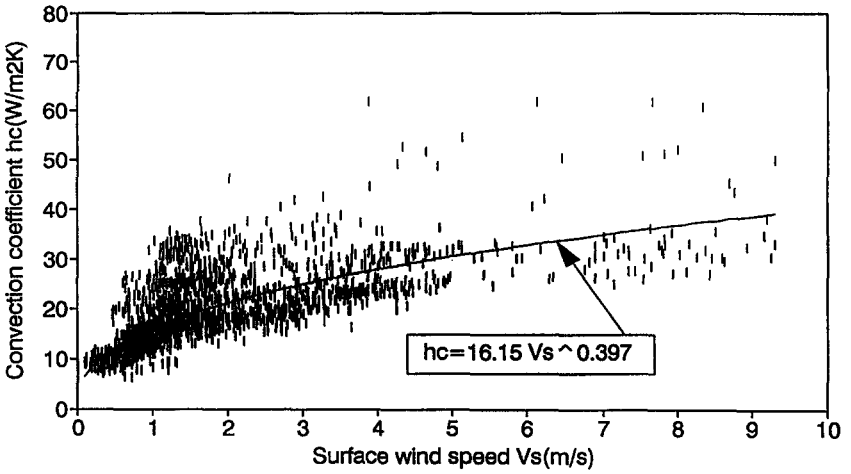

Fig. 13. Convection coefficient h_c vs surface wind speed V_s for windward conditions.

are seen to be lower than those for the windward conditions (also evident from Fig. 9). This is considered to be the result of the sheltering effect of the building. As expected, the correlation between h_c and V_s is significantly better than that for h_c and V_r for windward flow, due to the proximity to the test panel of the measuring position for V_s. In addition, the polynomial format of the above expressions is in agreement with that of theoretical expressions for convective heat transfer from a heated flat plate. The authors are currently determining a suitable dimensionless form for correlating Nusselt and Reynolds numbers, which will be applicable to full-scale building facades.

5.3. *Relationships between* V_s *and* V_r

Figures 15 and 16 illustrate the relations between wind speed V_s near the surface and wind speed V_r above the roof, for 'windward' and 'leeward' categories, respectively.

Figure 15 is plotted for conditions defined as 'windward' (i.e. 0°–180°). However, inspection of the plot clearly shows the emergence of two distinct regimes. Data in the lower part of the plot can be fitted by the linear regression:

$$V_s = 0.2V_r - 0.1 \tag{20}$$

and is considered to be the result of leeward-type (i.e. wake) flow conditions. These are caused by separation of the flow at the edges of the building when the incidence angle of the wind is close to either 0° or 180°; these findings agree with the ranges 0°–20° and 160°–180° for this type of behaviour, as quoted by Cook [9]. Data in the upper part of the plot is fitted by the much steeper regression:

$$V_s = 0.68V_r - 0.5 \tag{21}$$

which relates to purely windward flows within the approximate range 20°–160°. Note that the lower regression line of Fig. 15 [equation (20)] agrees closely with the regression line from Fig. 16 ($r = 0.86$):

$$V_s = 0.157V_r - 0.027 \tag{22}$$

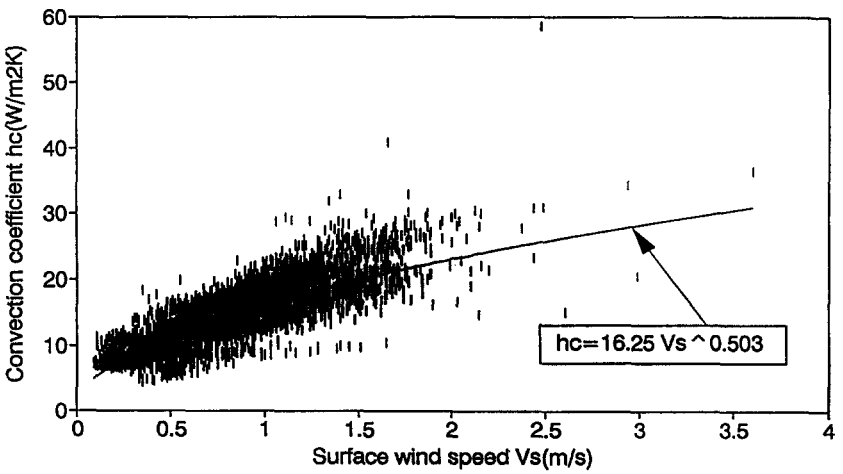

Fig. 14. Convection coefficient h_c vs surface wind speed V_s for leeward conditions.

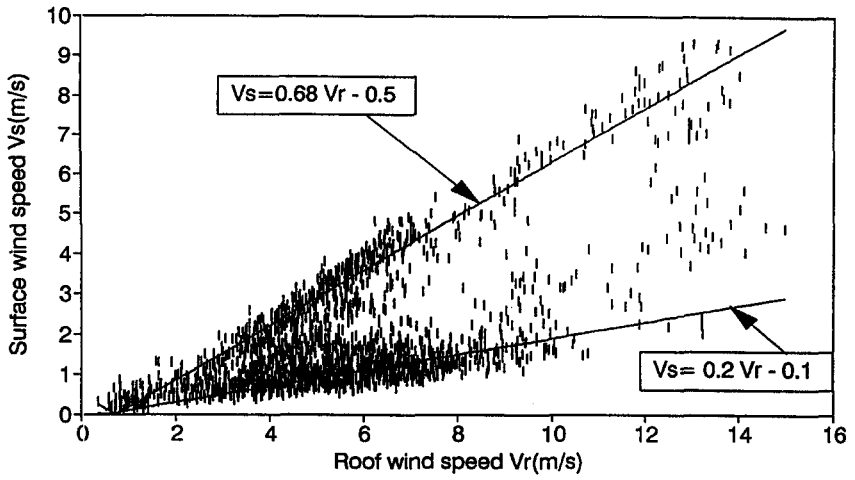

Fig. 15. Surface wind speed V_s vs roof wind speed V_r for windward conditions.

the latter relating to flow conditions known to be of a purely leeward, or wake, nature. Thus, while flow may be categorised as either 'windward' or 'leeward' upon solely azimuthal grounds, designers should in practice exercise caution in determining whether the flow is actually of a 'windward' or 'leeward' nature for any particular situation.

5.4. *Comparisons with other studies*

Figure 17 shows the comparison between h_c and surface wind speed V_s for the average correlation (19) based on the combined data from windward and leeward (categorised or azimuth) conditions, and is compared with results of previous investigations. It can be seen that the current study produces results which are consistent with those of earlier studies. Note that the results of the ASHRAE Task Group [7] are based on the work of Ito [3] which in turn relates to measurements at the sixth floor level of an L-shaped rectangular slab building in Tokyo. Both this and the present results give higher h_c values than either the CIBS [8] curve or that of Sharples [2]. In the latter case, the results from the 18th floor were taken for comparison purposes, since these gave the highest values for h_c as measured by Sharples [2].

Figure 18 shows the plots for h_c vs roof wind speed V_r, for windward conditions, and compares results with those from other investigators. Note that to make these comparisons, it was necessary in some instances to take V_{10} as the roof wind speed V_r. The current study is shown to give very good agreement with the ASHRAE [7] results; the other studies give markedly varying predictions for h_c. Figure 19 gives the corresponding results to Fig. 18, but for the leeward conditions; here, the present study, together with those of ASHRAE [7] and Sharples [2], give similar predictions for h_c, particularly at lower roof wind speeds. Only the CIBS findings [5] produce widely different predictions. Exact reasons for the variations in h_c predictions among the studies cannot be given, but differences in the microclimates around the individual test buildings, the geometries of the buildings

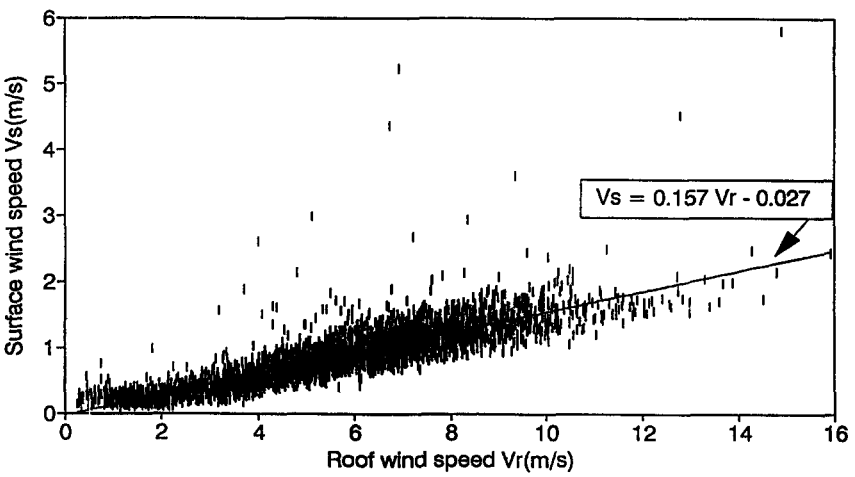

Fig. 16. Surface wind speed V_s vs roof wind speed V_r for leeward conditions.

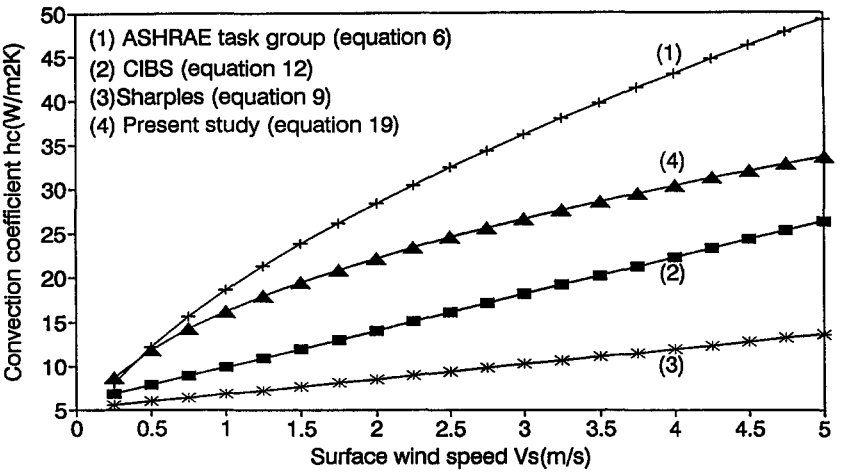

Fig. 17. Convection coefficient h_c vs surface wind speed V_s for combined windward and leeward conditions: comparison of this with other studies [2,7,8].

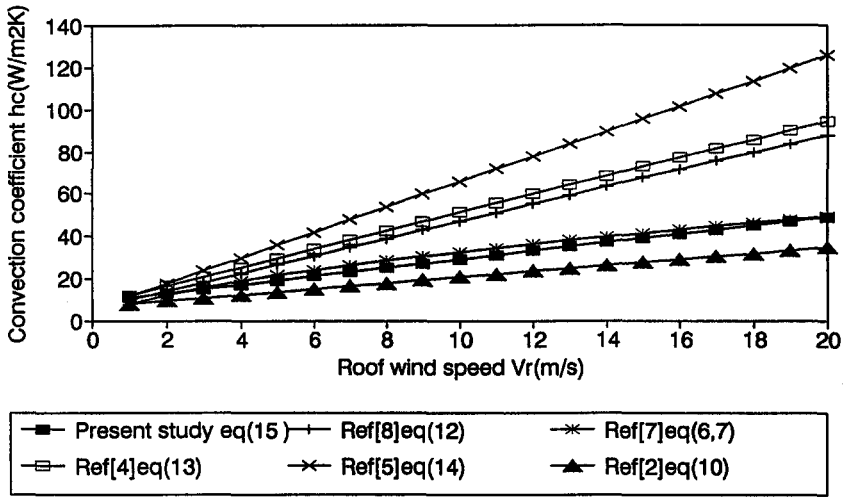

Fig. 18. Convection coefficient h_c vs roof wind speed V_r for windward conditions: comparison of this with other studies [2,4,5,7,8].

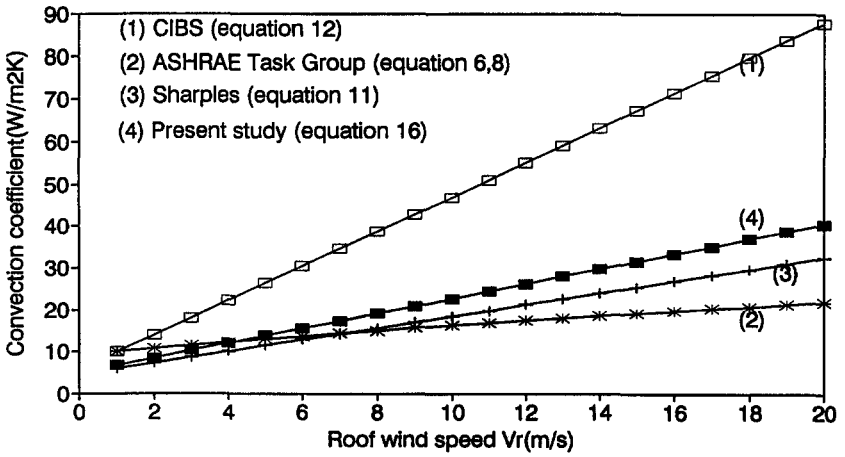

Fig. 19. Convection coefficient h_c vs roof wind speed V_r for leeward conditions: comparison of this with other studies [2,7,8].

themselves, as well as differing measurement conditions are the most likely causes. The conditions of application for the results presented in this paper are described next.

5.5. *Conditions of application*

Equations (15)–(18) inclusive can be used by designers to estimate values for the average external convection coefficient, h_c, of smooth-textured (glazed, metallic or acrylic, for example) surface elements at or near 0.8 m wide × 0.5 m high. The correlations are valid for elements within the central region of the wider facades of multi-storey cuboidal buildings between 4th and 8th floor levels; since the results were obtained in a semi-urban environment, the correlations can be used in conjunction with the Davenport [10] power law expression for windspeeds in semi-urban terrain.

Neither the position nor the height above ground of the test panel was varied in this study, either of which would have an influence on any derived correlations. However, Sharples [2] measured values for h_c as a function of windspeed at different heights and at centre and edge positions on the wider facade of an eighteen-storey cuboidal office in Sheffield city centre, U.K. His findings showed that h_c is greater at the edges than at the centre, and at the upper floors compared with the lower floors; in addition, he obtained reduced scatter (and hence better correlations) at the upper floors, as might be expected (increased disturbance to flow at the lower floors).

The nature of the flow in the atmospheric boundary layer near to the earth's surface is different for daytime and for night-time conditions (Stull, [11]). In this study, all results were taken at night; hence, the findings relate to those in a stably-stratified nocturnal boundary layer, especially those obtained at the lower wind speeds. It is possible, however, that results obtained at the higher wind speeds will correspond more closely to day-time mixed flow conditions. Hence, the correlations (15)–(18) may be used with greater reliability at the higher wind speeds if it is wished to predict h_c under day-time conditions (when wind speeds and thus convective heat loss rates will be greater).

The test panel comprised the upper surface of a cuboidal polypropylene box of depth 65 mm, so that when fitted to the building facade, this produced a 'step' between the wall surface and the panel surface. Such a configuration was necessary in order to:

(i) physically fix the panel to the wall surface while at the same time permitting easy access from the roof for the subsequent addition of surface disruptions (see below), and

(ii) to remain clear of local surface roughness effects produced by the brick wall of the building.

In order to minimise step-induced disturbance to the flow, the step height was kept to a minimum, and aluminium ramps were fitted to all four sides of the test panel. These will cause an acceleration in the air flow over the test surface, as compared with an unstepped arrangement, and thus a corresponding slight increase in the measured values for h_c can be expected. However, the variability in our values for h_c as measured will exceed any influence that the ramps will have upon these h_c values; it is therefore considered that the correlations as presented may be applied to flat facades with comparatively little error.

The authors are currently investigating the use of vertical strips to disrupt airflow across the test panel. This has implications for influencing convective heat loss from buildings. This is particularly relevant for windows, since the aim of the work is to optimise the framework geometry for glazing so as to reduce h_c and hence reduce energy losses. Wind tunnel studies have given encouraging results [12] by showing a reduction in h_c compared with a smooth surface for certain height : spacing ratios of window mullion. If similar reductions are observed in full-scale, it could form the basis of a flow management technique for reducing convective heat loss from glazing, in both retrofit and new-build applications. The results presented here will provide the basis for further comparisons. At present, equations (15)–(18) inclusive can be used for general prediction of h_c values for smooth facades.

6. CONCLUSIONS

Convective heat transfer coefficients have been measured for the case of a flat, undisrupted test panel located centrally at the sixth floor level of an 8-storey building. Values for heat transfer coefficients h_c have been correlated with wind speeds as measured at two locations: (a) in the free stream, 11 m above the roof of the building and (b) 1 m from the surface of the test panel.

(1) The correlation equations obtained were compared with those in the existing literature, and results were found to be consistent with those as reported in previous studies. Individual differences between studies are likely to be the result of differing building geometries, microclimates and measurement conditions. Turbulence intensity might help to specify particular conditions; this was not measured in the present study, and it is recommended that such measurements are carried out in future work in this field.

The correlations presented in this study are considered to be of good quality and accuracy, for the following reasons. Firstly, an ultrasonic anemometer was employed, giving a reading of V_s to an accuracy of $\pm 3\%$. The ultrasonic anemometer is purpose-designed for omni-directional velocity measurement in an external environment; previous workers have not used such sophisticated equipment. Secondly, the use of one panel only in the present study has been shown by uncertainty analysis to be potentially more

accurate than the use of two panels. Thirdly, the heat flux plate employed is of a continuous laminar design offering greater uniformity and sensitivity than that of the thermopile systems used previously by others.

(2) Shelter effects of the building are found to reduce the values of h_c for wind flows from the leeward direction compared with the windward direction. In this study, the highest convection losses occur when the angle of wind incidence lies between 125 and 150° to the test facade. This corresponds to the prevailing wind direction for the locality, namely south-west. This might offer some guidance as regards applicability to other buildings, though local microclimate effects must always be considered. In particular, designers should exercise caution when categorising wind flow as 'windward' or 'leeward' around a particular building; flow separation at building edges should be taken into consideration in all cases.

(3) The correlation equations (15)–(18) inclusive can be used in thermal models and by designers to estimate values for the average external convection coefficient, h_c of smooth-textured (glazed, metallic or acrylic, for example) undistrupted surface elements at or near 0.8 m wide × 0.5 m high; the expressions are valid for elements within the central region of the wider facades of multi-storey cuboidal buildings between 4th and 8th floor levels inclusive. They may be used to estimate values for h_c for similar buildings in a semi-urban setting in conjunction with the Davenport [10] power law expression for wind flows in semi-urban environments.

Acknowledgements—This work was funded by the U.K. Science and Engineering Research Council, to whom the authors express their gratitude. The authors thank Mr H. Versteeg, Loughborough University of Technology and Dr S. Sharples, Sheffield University, for helpful discussions. The provision of aerial photographs by the Loughborough Students Union Hot Air Balloon Club is gratefully acknowledged.

REFERENCES

1. The Chartered Institution of Building Services Engineers (CIBSE), *Guide A*. CIBSE, London (1986).
2. S. Sharples, Full-scale measurements of convective energy losses from exterior building surfaces, *Building Envir.* **19,** 31–39 (1984).
3. N. Ito, K. Kimura and J. Oka, A field experiment study on the convective heat transfer coefficient on exterior surface of a building. *ASHRAE Trans.* **78,** 184–191 (1972).
4. K. Nicol, The energy balance of an exterior window surface. Inuvik, N.W.T., Canada, *Building Envir.* **12,** 215–219 (1977).
5. N. S. Sturrock, Localised boundary layer heat transfer from external building surfaces, Ph.D. Thesis, University of Liverpool (1971).
6. J. A. Duffie and W. A. Beckman, *Solar Energy Thermal Process*. John Wiley, New York (1974).
7. ASHRAE Task Group, *Procedure for Determining Heating and Cooling Loads for Computerising Energy Calculations. Algorithms for Building Heat Transfer Subroutines*. ASHRAE Publications, New York (1975).
8. *CIBS Guide Book A*, Section A3, CIBS, London (1979).
9. N. J. Cook, *The Designer's Guide to Wind Loading of Building Structures*: Part 2 *Static Structures*. Building Research Establishment/Butterworths, London (1990).
10. A. G. Davenport, The treatment of wind loading on tall buildings, *Proceedings of Symposium on Tall Buildings*, University of Southampton, U.K. (1966).
11. R. B. Stull, *An Introduction to Boundary Layer Meteorology*. Kluwer Academic, Dordrecht (1988).
12. D. L. Loveday, P. A. Bosanquet and C. M. Stainforth, The effect of surface disruptions on the convective heat loss from glazing, *ASHRAE Trans.* **97,** 82–89 (1991).